Elementary excitations in liquid ^{4}He confined in MCM-41

Francesco Albergamo*
Laboratoire Léon Brillouin, CEA Saclay, 91191 Gif-sur-Yvette Cedex, France
and Istituto Nazionale di Fisica della Materia, Unità dell'Aquila, Italy

Jacques Bossy†
Centre de Recherche sur les Très Basses Températures, CNRS, Boîte Postale 166, 38042 Grenoble Cedex 9, France

Henry R. Glyde‡
Department of Physics and Astronomy, University of Delaware, Newark, Delaware 19716-2570, USA

Albert-Jose Dianoux§
Institut Laue-Langevin, Boîte Postale 156, 38042 Grenoble, France
(Received 24 January 2003; published 13 June 2003)

We present neutron scattering measurements of the excitations of liquid ^{4}He confined in MCM-41 at wave vectors 0.35 Å$^{-1} \leqslant q \leqslant$ 2.15 Å^{-1}. MCM-41 is a uniform porous material consisting of cylindrical pores, here of 32 Å diameter. The location and phase of ^{4}He in the pores was well characterized by pressure isotherms and by exploratory neutron scattering measurements. The first 60% of ^{4}He entering the MCM-41 is tightly bound on the media surface. This ^{4}He supports no excitations in the energy range investigated (0.3 meV $\leqslant \omega \leqslant$ 2.0 meV). The ^{4}He added between 60 and 70% filling is less tightly bound. At 70% filling, ^{4}He in MCM-41 supports an excitation that is interpreted as a ripplon propagating on the liquid surface. This excitation disappears on further filling. The subsequent liquid ^{4}He added supports well defined phonon-roton excitations which at low temperatures $T \leqslant 1.4$ K, have energies and widths that are the same as those in bulk superfluid ^{4}He within precision. There is some indication that the phonon energy for $q \leqslant 0.5$ Å^{-1} lies above the bulk value. The liquid also supports layers modes for wavevectors in the roton region (1.90 Å$^{-1} \leqslant q \leqslant$ 2.15 Å^{-1}) as observed in aerogel, Vycor, and Geltech silica. Accurate measurements at higher temperatures were not possible because of the small volume of liquid in the MCM-41 and the present sample cell design.

DOI: 10.1103/PhysRevB.67.224506 PACS number(s): 67.40.Yv, 67.70.+n, 68.03.Kn, 61.12.−q

I. INTRODUCTION

The impact of disorder on Bose-Einstein condensation (BEC), on the elementary excitations and on superfluidity of Bose systems is a topic of great current interest. Liquid ^{4}He immersed in porous media is the most accessible example of bosons in disorder.[1–3] Other topical examples are Cooper pairs of electrons and flux lines in high-T_c superconductors,[2,4–6] Josephson Junction arrays, and disordered thin films.[7]

The superfluid properties of helium confined in several porous media have been extensively investigated.[1] In disorder, many superfluid properties are substantially modified. For example, the critical temperature of the normal liquid to superfluid transition T_c is lowered. The smaller the pore size of the media the further T_c is lowered below the bulk value $T_\lambda = 2.17$ K. Also, the temperature dependence of the superfluid density $\rho_s(T)$ below T_c can be modified by disorder. For example, the critical exponent ζ describing $\rho_s(T)$ in aerogel differs from the bulk value. This result have been confirmed in several macroscopic measurements[8–12] on ^{4}He confined in aerogels. This places ^{4}He in aerogel in different *universality class* from the bulk. However, Maynard and Deutscher[13] showed that the observed ζ value could be interpreted as an effective value averaged over the actual pore size distribution of the confining material.

At very low filling of the media, ^{4}He appears to behave as a dilute Bose gas of atoms attached to the media walls.[14] For example, at low coverage, T_c follows the density dependence expected for a dilute Bose gas. The physics of ^{4}He at low coverage is quite different from that of the liquid ^{4}He that forms near full filling of the pores.

More recently, the elementary phonon-roton and other excitations of liquid ^{4}He in several porous media have been investigated by inelastic neutron scattering. Examples are liquid ^{4}He in aerogel,[15–25] in xerogel,[26,27] in Vycor,[25,28,29] and in Geltech silica.[30,31] At or near full filling of the pores, the phonon-roton energies and linewidths are the same as in bulk liquid ^{4}He, unchanged by disorder within current precision (± 5 μeV). Some differences have been reported but improved precision and direct comparison with the bulk under the same experimental conditions shows that they are the same. Specifically, the temperature dependence of the excitation energies and the widths are the same as in the bulk.[24,25] At partial fillings there is some difference in the energies[24] suggesting that the density of liquid ^{4}He near a free surface is lower than the bulk value.

In porous media there are, in addition, two dimensional modes propagating in the liquid ^{4}He layers adjacent to the media walls.[24,25,28,31] These additional ''layer modes'' are observed unambiguously at wave vectors in the roton region only, although they may exist with weaker intensity at lower wave vectors. These modes appear to be the same as those observed in ^{4}He films adsorbed on graphite.[32] The layer modes also appear to be responsible for the difference in the

thermodynamic properties of ^{4}He in porous media and the bulk, in Vycor, for example.[25,29]

Rather unexpectedly, phonon-roton excitations of superfluid ^{4}He are observed at temperatures above T_c in Vycor and Geltech silica, up to T_λ. Since the existence of well-defined excitations at higher wave vectors is attributed to the existence of a condensate, this observation suggests that there is BEC above T_c in porous media.[31,33] This BEC is probably localized to specific regions in the porous media by the disorder so that there is phase coherence over short length scales only rather than across the whole sample as needed for superflow. Direct measurement of BEC in Vycor by high-energy inelastic neutron scattering has also now begun.[34]

In this paper we present measurements of the elementary excitations of superfluid ^{4}He in MCM-41, a porous media consisting of regular cylindrical pores of well defined diameter, here 32 Å. The aim is to determine the excitations in a media having small diameter pores to increase the effects of confinement and disorder. In addition MCM-41 has a narrow pore size distribution so that the degree of confinement is quite uniform throughout the sample. We also characterize the MCM-41 more carefully than has been done in the past using N_2 and ^{4}He pressure isotherm measurements, x-ray measurements, and preliminary neutron scattering measurements. With these techniques we have determined the pore diameter of the MCM-41 accurately and the state of the ^{4}He in the pores as a function of filling of the media. Specifically, the filling at which liquid forms in the MCM-41 was clearly identified. With this data, we can relate unambiguously the character of the observed neutron scattering data with state of the ^{4}He in the MCM-41 pores. We focused on measurements at low temperature as a function of filling of the media. In addition, we employed a sample cell design that prevented the formation of liquid ^{4}He elsewhere in the cell. In this way the observed neutron scattering intensity could be reliably correlated with the degree of filling of the MCM-41.

In Sec. II we describe the synthesis and characterization of the MCM-41. The neutron scattering measurements are presented and analyzed in Sec. III. A discussion and summary is presented in Sec. IV.

II. SAMPLE CHARACTERIZATION

A. MCM-41 synthesis

The MCM-41 used in the present research was synthesized by the group of Patarin and Soulard at the ''Laboratoire de Matériaux Minéraux,'' Mulhouse, France, following the prescription described by Corma, Kan, Navarro, Pérez-Pariente, and Rey.[35] The sample, in the form of a white powder of μm size, has a measured density of 0.269(5) g/cm^3. Nitrogen adsorption-desorption isotherm measurements at 77 K were perfomed by them using commercial equipment. A standard treatment of these isotherms within the Barrett, Joyner, and Halenda (BJH) model[36] was made to determine the pore size. This yielded a distribution of pore diameters that was sharply peaked at 32 Å and had a very narrow width; a full width at half maximum (FWHM) $\simeq 3$ Å. We stress that the average pore size is dependent upon the model used to describe the data (BJH in this case). The narrowness of the pore size distribution is somewhat more reliable. The surface area of the MCM-41 obtained in the framework of the Brunauer, Emmett, and Teller (BET) theory[37] from the isotherm data was $s=910$ m^2/g. The N_2 pressure isotherms show evidence of capillary filling. Capillary filling is characterized by some upward curvature and hysterisis of the absorption and desorption curves. It is believed to be associated with filling as liquid N_2 in which surface tension plays an assisting role. They also measured the x-ray diffraction pattern of the MCM-41 and obtained results for the pore sizes that are consistent with the above determination.

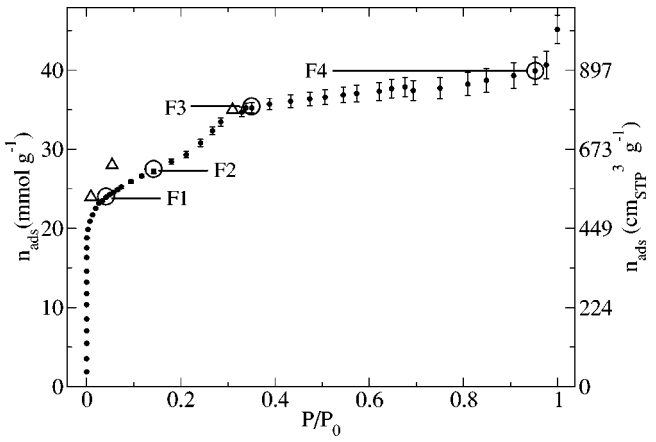

FIG. 1. Helium adsorption diagram at $T=2.48\pm0.01$ K (filled circles with error bars). Open triangles represent isothermal data taken at $T=1.20\pm0.01$ K, while open circles represent the fillings chosen for neutron scattering experiments, namely, F1: 24 mmol/g; F2: 28 mmol/g; F3: 35 mmol/g; and F4: 40 mmol/g.

B. MCM-41 characterization by ^{4}He isotherms

To determine how ^{4}He atoms fill MCM-41, we conducted helium adsorption isotherm measurements at a temperature of 2.48(1) K. The equipment used is a series of steel calibrated volumes over which we measured the pressure by capacitance barometers. The cryostat used is of the *orange* type.[48] The sample was outgassed at a temperature of about 330 K until a residual pressure of 3.3×10^{-4} mbar was reached.

The resulting ^{4}He adsorption isotherm is displayed in Fig. 1 and is interpreted as follows. A large amount of ^{4}He is adsorbed initially by the MCM-41 at very low pressure. That is, up to filling F1=24 mmol/g, indicated by an open circle in Fig. 1, the ^{4}He is adsorbed at a low pressure P relative to the saturated vapor pressure (SVP) of bulk liquid ^{4}He P_0 of $P/P_0\leqslant0.05$. The ^{4}He entering the MCM-41 up to filling F1 is therefore tightly bound to the media surface and forms one or more layers on the surface. A BET analysis would show the first monolayer completed at filling F1 but this could include some tightly bound ^{4}He in a second layer. The first ^{4}He layer is generally believed to be solid. Between fillings F1 and F2 in Fig. 1, the ^{4}He is still reasonably tightly bound ($P/P_0\leqslant0.14$), but somewhat less so. Between fillings F2

and F3, the MCM-41 cylindrical pores are being filled by liquid and the upward curvature in the isotherm suggests capillary condensation. The capillary filling of the cylinders is completed at filling F3. The filling of the porous sample itself, including larger pores and, in general, less favorable adsorption sites including compressing existing phases, is completed at F4. Beyond filling F4, the ^{4}He entering the sample is interpreted as filling the spaces between the grains in the powder with liquid at almost SVP.

To construct a simple model of the ^{4}He in MCM-41, we assume that two solid ^{4}He layers form on the MCM-41 surface. We assume also that the surface density n for these ^{4}He layers as well the interatomic spacing a within these layers is the same as observed for ^{4}He on graphite,[32,38–40] namely, $n_1=0.115$ atoms/Å^2 ($a_1=3.17$ Å) for layer 1 and $n_2=0.095$ atoms/Å^2 ($a_2=3.54$ Å) for layer 2. Finally we assume that the liquid phase obtained after the two layers have formed, has the bulk lower lambda point density, namely $\rho_\lambda=0.022$ Å^{-3}.

Using a cylinder diameter of $d=32$ Å , the diameter of the ring formed by the centers of the ^{4}He atoms in the first layer is $d_1=d-a_1=28.83$ Å . Similarly, the nitrogen monolayer forms on a cylindrical ring whose diameter is $d_1^{N_2}=d-d_{N_2}$, where d_{N_2} is the diameter of the N_2 molecule used in the BET analysis, namely $d_{N_2}=4.33$ Å . Using the surface area of the cylinders obtained from N_2 isotherms of $s=910$ m^2/g, the number of atoms expected in the first helium layer is $N_1=s_1n_1=18.1$ mmol/g, where $s_1=(d_1/d_1^{N_2})s=948$ m^2/g. The diameter of the cylindrical surface on which the second layer forms is $d_2=d_1-a_1-a_2=22.12$ Å and the surface area available to the second layer is $s_2=(d_2/d_1)s_1$. The number of atoms in the second layer is $N_2=s_2n_2=11.5$ mmol/g. Thus the total in the two layers is $N_{lay}=N_1+N_2=29.6$ mmol/g which is consistent with filling F2=28 mmol/g in Fig. 1.

Particularly the surface density of ^{4}He on MCM-41 could be less than that on graphite. In this picture, the width of each layer is taken equal to the interatomic spacing, the resulting three-dimensional layer densities are $\rho_1=0.0363$ Å^{-3} and $\rho_2=0.0268$ Å^{-3}, yielding an average density for the layered helium of $\bar{\rho}_{lay}=(\rho_1V_1+\rho_2V_2)/(V_1+V_2)=0.0319$ Å^{-3}, where V_1 and V_2 are the volumes occupied by the first and second layer.

The remaining ^{4}He then enters the MCM-41 as liquid until the cylinders are full. With two solid ^{4}He layers added, the diameter of the remaining volume in the cylinders available to the liquid is $d_{liq}=d_2-a_2=18.58$ Å . The ratio of the liquid volume to layer volume is therefore 0.51 while the ratio of liquid density to layers average density is 0.69. A liquid amount of $N_{liq}=0.51\times0.69\ N_{lay}=10.4$ mmol/g is then expected to fill the cylinders. This agrees well with the amount of liquid suggested by the isotherms in Fig. 1; F4 $-$F2=12 mmol/g. Thus this simple picture is consistent with the observed ^{4}He isotherms.

To construct the above simple model, we have assumed that the first two layers are solid layers. The second solid layer could equally well be partly or wholly dense liquid, as suggested by the data to follow.

TABLE I. Experimental conditions for the neutron scattering experiment performed on MIBEMOL spectrometer.

filling	T (K)	$SVP(T)$[a] (mbar)	P[b] (mbar)	n_{ads} (mmol g^{-1})
0	1.20(2)	0.81(1)	0.000 33(1)	0
F1	1.20(2)	0.81(1)	0.001 96(1)	23.3(3)
F2	1.20(2)	0.81(1)	0.030 10(6)	28.1(4)
F3	1.20(2)	0.81(1)	0.2356(4)	36.1(4)
F4	1.32(2)	1.79(2)	1.788(3)	39.8(5)

[a]Saturated vapor pressures are taken from literature (Ref. 41).
[b]The pressure has been corrected for thermomolecular effects with the Weber Schmidt formula (Ref. 42).

C. MCM-41 characterization by inelastic neutron scattering

In order to further characterize the filling of MCM-41 by ^{4}He, we made preliminary measurements of the inelastic neutron scattering (INS) intensity as a function of filling. The measurements were carried out at a fixed sample temperature of $T=1.20(2)$ K on the MIBEMOL time of flight spectrometer at the Laboratoire Léon Brillouin (LLB), Saclay, France. The goal was to identify the qualitative features of the excitations supported by the ^{4}He in the MCM-41 at particular fillings. Specifically, the INS intensity at five fillings was measured. These were an empty MCM-41 sample and the four fillings F1 to F4 identified in Fig. 1. The fillings are summarized in Table I.

The sample cell was an aluminum cylinder (outer diameter 17 mm, inner diameter 16 mm), glued with stycast to a flange. The flange was connected to the cryostat injection pipe via an indium joint. The cell was filled with 758.4 mg of MCM-41. This was outgassed at 370 K until a pressure of 3.4×10^{-4} mbar was reached prior to filling. A fixed incident neutron wavelength of $\lambda=5$ Å was used and the data was collected at constant scattering angle. In order to improve the statistics, data at several scattering angles were combined. Specifically, we report in Fig. 2, the net INS intensity collected at scattering angles in the range (a) 69.2°–80.6°, (b) 84.5°–95.5°, (c) 100.5°–111.8°, (d) 117.0°–141.8°. These angles correspond to wave vector transfers at the elastic line in the range (a) 1.43–1.62 Å^{-1}, (b) 1.69–1.86 Å^{-1}, (c) 1.93–2.08 Å^{-1}, and (d) 2.14–2.37 Å^{-1}. Since the data was taken at $T=1.20$ K, the actual ^{4}He vapor pressure above the sample does not fall exactly on the $T=2.48$ K isotherm shown in Fig. 1. The actual vapor pressure in the INS measurement at fillings F1, F2, and F3 are shown as triangles in Fig. 1. It should be noted also that at the 40 mmol/g filling, there were indications that some of the helium was condensing into the cryostat injection pipe. We must conclude that the actual filling was not fully 40 mmol g^{-1}, but a somewhat lower filling.

The observed INS intensity is shown in Fig. 2. The chief findings are well represented by (c) of Fig. 2. The INS signal at filling F1 (24 mmol g^{-1}) is not distinguishable from the

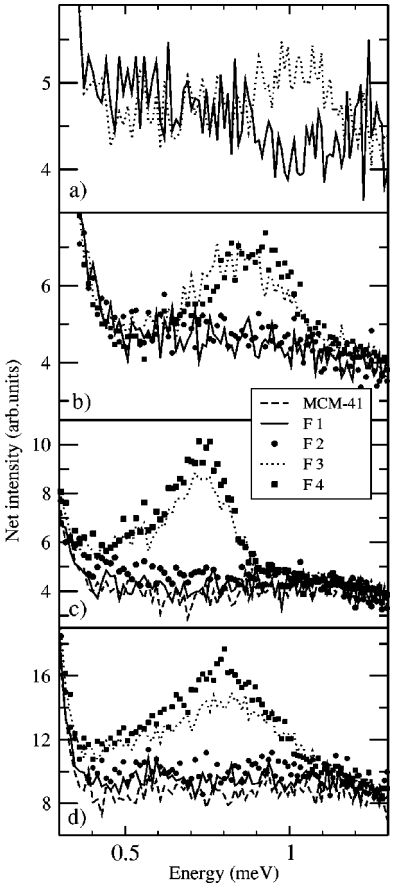

FIG. 2. Raw inelastic neutron scattering spectra obtained with the MIBEMOL spectrometer. The four panels show four different ranges of exchanged elastic wave vector $q_{\mathrm{el}} \equiv q(\omega=0)$: (a) $q_{el}=(1.52\pm0.10)$ Å^{-1}, (b) $q_{\mathrm{el}}=(1.78\pm0.08)$ Å^{-1}, (c) $q_{\mathrm{el}}=(2.00\pm0.08)$ Å^{-1}, (d) $q_{\mathrm{el}}=(2.26\pm0.12)$ Å^{-1}.

empty MCM-41 signal in the energy range shown. This suggests that the helium up to filling F1 is tightly bound to surfaces of the MCM-41 and has excitations at a much higher energy. Up to filling F1, the ^{4}He forms at least one amorphous solid layer plus perhaps some liquid or solid domains in a second layer. At filling F2 (28 mmol g^{-1}) a weak, broad inelastic signal is observed. A similar weak, broad INS intensity was observed as the first signal from ^{4}He in 25 Å Geltech silica[30,31] at low fillings. This suggests that some of the less tightly bound ^{4}He in the second layer at F2 may be liquid. At filling F3 (35 mmol/g) a significant increase in INS intensity is observed. This is in the energy range expected for a roton and supports the interpretation that filling between F2 and F3 is liquid ^{4}He. The inelastic signal at filling F4 (40 mmol g^{-1}) is only marginally greater than that at F3. This may arise from the filling problems at F4 noted above. We then conclude that the phonon-maxon-roton signal arises from the liquid ^{4}He that capillary condenses between fillings F2 and F3.

In summary, the N_2 and ^{4}He pressure isotherms and the neutron scattering characterization suggest that the MCM-41 consists of 32 Å diameter cylindrical pores and has a surface area of 910 m^2/g. At ^{4}He filling F1=24 mmol/g, all the ^{4}He is tightly bound to the MCM-41 walls mainly in solid layers.

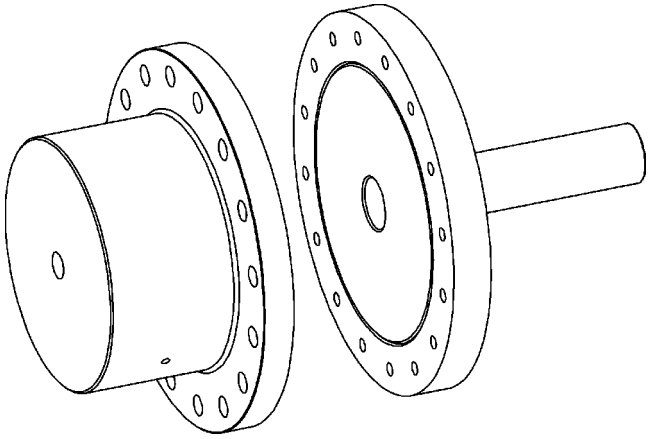

FIG. 3. Sample cell for the neutron experiment on IN6. On the right, the aluminum part, containing the MCM-41 sample, on the left the brass part providing the open volume needed to correctly fill the porous sample with helium. An indium joint has been used to connect the two parts.

There is no observed inelastic response from the solid layers. Between filling F1 and F2=28 mmol/g, the ^{4}He layers are less tightly bound and there is weak, broad inelastic response from this (possibly liquid) ^{4}He. Between F2 and F3=35 mmol/g, the ^{4}He enters as liquid which supports phonon-roton excitations. Beyond F3, the ^{4}He added up to F4=40 mmol/g (full cylinders) is also liquid but the magnitude of the INS intensity from this ^{4}He was not well determined.

III. NEUTRON SCATTERING DATA

In this section, we present neutron scattering measurements of the excitations of ^{4}He in MCM-41 taken on the time of flight IN6 spectrometer at the Institut Laue-Langevin (ILL), Grenoble, France. Measurements were made at three fillings of the MCM-41: empty MCM-41, filling F2 shown in Fig. 1 which corresponds to completed ^{4}He layers on the MCM-41 surfaces and filling F3 which corresponds to completed filling with liquid by capillary condensation. For this experiment we chose an incident wavelength of $\lambda=4.62$ Å . A ^{3}He cryostat was used to reach temperatures as low as 0.35 K.

A. Sample cell design

In order to avoid any condensation of bulk liquid ^{4}He in the injection tube of the cryostat, we designed a special sample cell (see Fig. 3). The cell consisted of two parts. One part was an aluminum cylinder of inner diameter 15 mm and wall thickness 1 mm which held the MCM-41. The other was a brass open volume (approximately 115 cm^3). The two parts are sealed together by an indium joint. The MCM-41 was outgassed at 370 K until a pressure of 10^{-4} mbar was reached. ^{4}He gas was then added to the brass volume at room temperature and the copper injection pipe was sealed by a cold seal technique. Two such cells were constructed, cells A and B. Cell A, whose open volume is 114.9(4) cm^3, was filled with sufficient ^{4}He gas [11.45(4) bar] so that when cooled in the cryostat, the amount of ^{4}He adsorbed by the

TABLE II. Experimental conditions for the neutron scattering experiment performed on the IN6 spectrometer.

cell	T (K)	$P_0(T)$ [a] (mbar)	n_{ads} (mmol g^{-1})
A	0.41(1)	$5\cdot10^{-7}$	28.08
A	25.00(5)		≈ 0
B	0.388(4)	$2.0\cdot10^{-7}$	36.15
B	1.016(16)	0.20	36.10
B	1.200(1)	0.81	35.95
B	1.400(1)	2.8	35.60
B	1.500(2)	4.8	35.35
B	1.600(1)	7.5	35.00
B	24.85(15)		≈ 0

[a]Saturated vapor pressure are taken from literature (Ref. 41).

MCM-41 [1.891(2) g] corresponded to a filling of F2=28 mmol/g. Cell B, whose open volume is 115.0(4) cm^3, was filled with ^{4}He gas [14.49(4) bar] so that the MCM-41 [1.860(2) g] was filled to filling F3=36 mmol/g when cooled. Once sealed, the actual filling of the MCM-41 is a function of temperature. The precise fillings in cells A and B at each temperature are given in Table II. Background measurements on empty MCM-41 measurements were made by heating the MCM-41 to 25 K.

B. General features

To display the general features of the excitations, we present the data as the net scattering intensity from ^{4}He in MCM-41 at fillings F2 (28 mmol/g) and F3 (35 mmol/g) relative to the empty MCM-41 intensity. The scattering intensity from the empty MCM-41 was the same for the two cells. Figures 4–6 show this net intensity at $T=0.4$ K for scattering wave vectors in the range $0.45\leqslant q\leqslant 2.10$ Å^{-1}. From Fig. 4 we see a structureless response at filling F2 for $q\leqslant 0.55$ Å^{-1}. At filling F2 and $q\geqslant 0.85$ Å^{-1} we observe a broad weak peak at $\hbar\omega\approx 0.7$ meV plus a high energy tail. At filling F3 and low temperature we observe a well defined peak, identified as the phonon-roton excitations, plus a high energy tail. The high energy tail is nearly identical at fillings F2 and F3 (Figs. 4 to 6) and for all temperatures studied (Fig. 7). Thus the high energy tail cannot be attributed to multiphonon processes, since it is equally present for filling F2 where a single excitation contribution is not present at all.

The peak observed at filling F2 has disappeared at filling F3, indicating that the excitation at F2 is destroyed once the pores are filled by capillary condensation. One interpretation is that the excitation at F2 is located at the boundary between the second layer and the vapor, constituting a so called ''ripplon.'' Such an excitation has already been observed on the surface of liquid layers of ^{4}He adsorbed on graphite.[32,43] Given the powder nature of the present MCM-41 sample, we cannot observe the ripplon energy dispersion curve.[44–46] Rather, we observe the ripplon density of states. Also, the cylindrical geometry of our system could modify the ripplon dispersion relation, originally calculated for a planar geometry. Substrate-surface interaction should modify the dispersion relation in the long wavelength regime only. The area of the liquid-vapor surface is greatly reduced at filling F3, since the pores are largely filled by liquid, thus explaining the loss of the ripplon signal at F3.

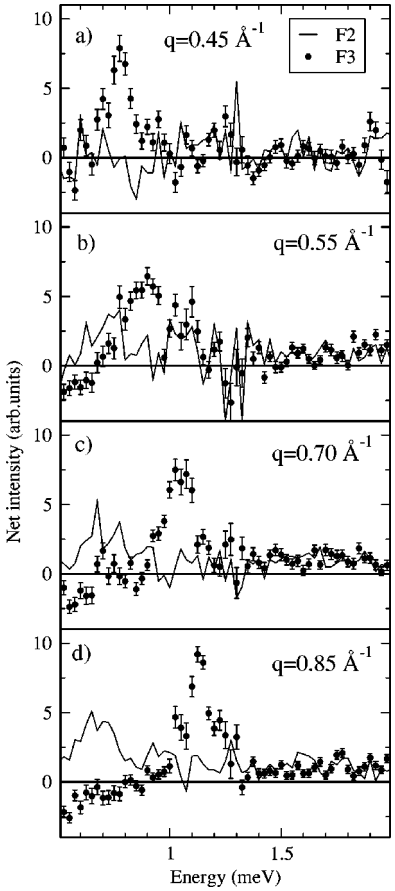

FIG. 4. Net scattering intensity from liquid ^{4}He in MCM-41 at $T=0.4$ K at fillings F2 (28.1 mmol g^{-1}) and F3 (36.1 mmol g^{-1}). Four wave vector transfers q in the ''phonon'' region are shown. Between filling F2 and F3, the ^{4}He fills the pores as liquid by capillary condensation.

C. Fitting

To analyze the phonon-roton excitations observed in the liquid at filling F3, we consider the net intensity observed between fillings F3 and F2. Particularly the high energy tail which is observed at both fillings F2 and F3 does not appear in the net intensity. However, the ''ripplon'' intensity that appears at filling F2 and not at F3 results in negative net intensity in this subtraction. To avoid this negative ''ripplon'' intensity we fitted the data in the energy range of the phonon-roton peak only. In the wave vector range where the ''ripplon'' and the phonon-roton peak overlap, we tried both filling F2 and the empty MCM-41 as background references. The resulting fits were found to converge better for the data sets referenced to the F2 signal. Examples of data obtained by subtracting the F2 signal with fits for several values of q at $T=0.4$ K are shown in Fig. 8.

As the fitting function, we used the convolution of previously measured experimental (Gaussian) resolution function with a damped harmonic oscillator (DHO) function

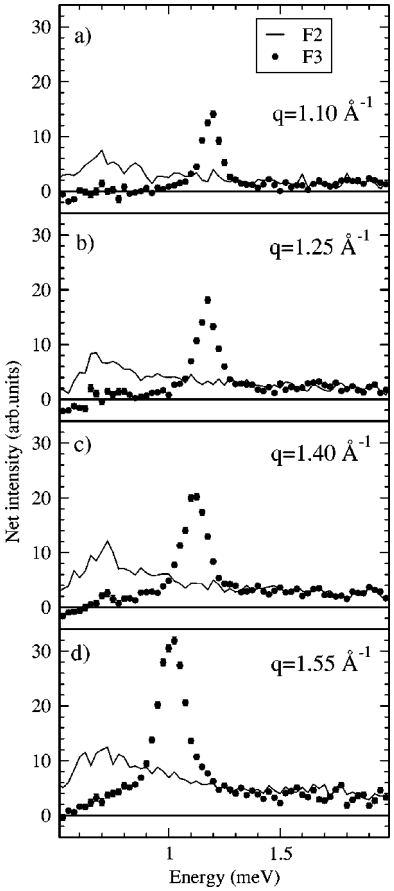

FIG. 5. Same as Fig. 4, for wave vector transfers in the ''maxon'' region.

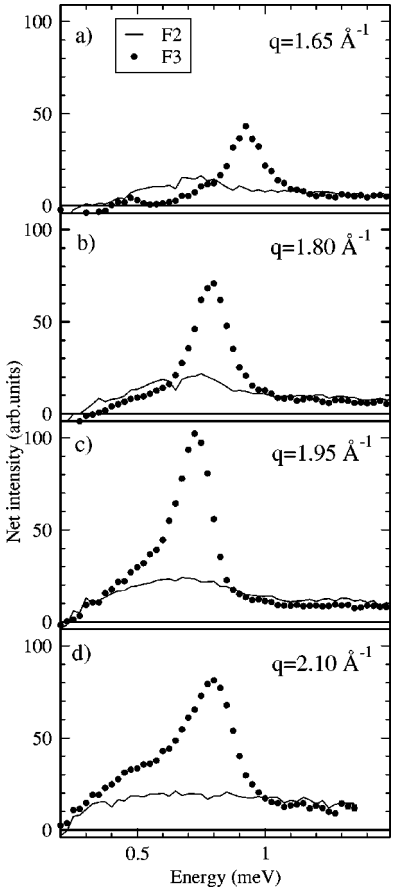

FIG. 6. Same as Fig. 4, for wave vector transfers in the ''roton'' region.

$$S_1(q,\omega)=\frac{Z_q[n_B(\omega)+1]}{\pi}\times\left\{\frac{\Gamma_q}{(\omega-\omega_q)^2+\Gamma_q^2}-\frac{\Gamma_q}{(\omega+\omega_q)^2+\Gamma_q^2}\right\}, \quad (1)$$

where

$$n_B(\omega)\equiv\frac{1}{e^{\beta\hbar\omega}-1} \quad (2)$$

is the Bose function. The ω_q, Γ_q, and Z_q are free fitting parameters representing the energy, half width, and intensity of the excitation, respectively. For $q>1.50$ Å^{-1}, we added a Gaussian

$$G(q)=\frac{A_q}{\sqrt{2\pi\,\sigma_q^2}}\,e^{(\omega-\omega_q^{2D})^2/2\sigma^2} \quad (3)$$

to the fitting function in order to take into account the 2D excitations. We found that $A_q=0$ for wave vectors up to $q=1.85$ Å^{-1}.

D. Dispersion

In Fig. 9 we show the phonon-roton energy dispersion curve, ω_q, obtained by fitting Eq. (1) to the peak region of $S(Q,\omega)$ at several q values. There we see that the phonon-roton energies of superfluid ^{4}He in MCM-41 agree well with those in the bulk[47] over most of the wave vector range. At low $q(q\leqslant 0.65$ Å$^{-1})$ the phonon energies ω_q in MCM-41 lie somewhat above the bulk values. Generally we expect finite size to affect excitations having wavelengths comparable or greater than the pore size. Particularly, long wavelength phonons propagating perpendicular to the cylinder axis are likely to be most affected by the finite size of the MCM-41.

The two dimensional (2D) layer modes were observed only for wave vectors in the roton region and beyond the roton. The energy ω_q^{2D} of this 2D mode is reasonably independent of q over the range that it is observed. A similarly flat dispersion curve for ω_q^{2D} was observed in 25 Å Geltech silica. In contrast, a parabolic dispersion curve for ω_q^{2D} was observed in Vycor and aerogel. At these wave vectors, roton and higher, the 3D phonon-roton ω_q in MCM-41 appears to lie somewhat below the bulk value. A similar difference from the bulk was observed in Geltech silica when it was not completely filled. However, there are difficulties in separating the scattering intensity arising from the 2D and 3D excitations uniquely at these wave vectors and this difference could arise from not assigning enough intensity to the 2D mode.

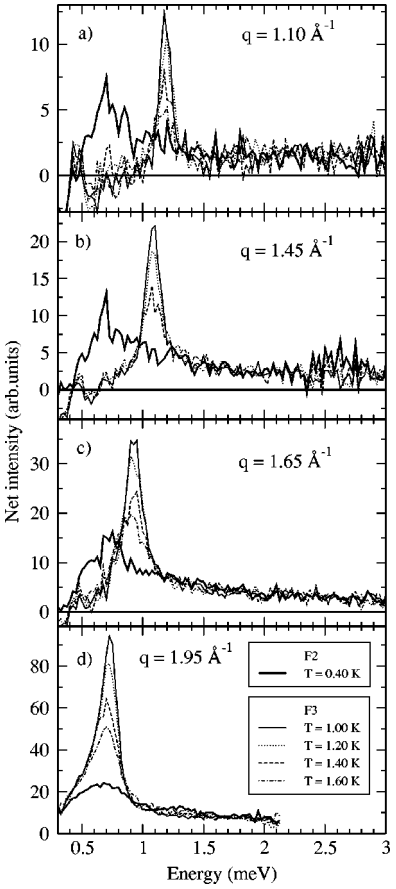

FIG. 7. Same as Fig. 4, for several temperatures at filling F3.

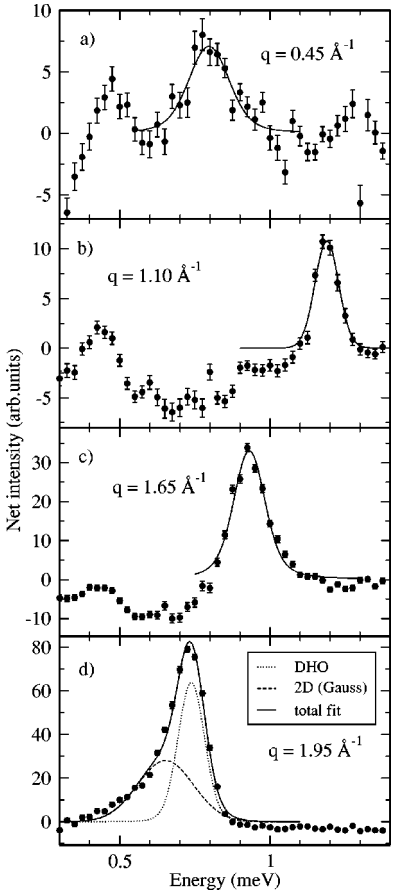

FIG. 8. Net scattering intensity from ^{4}He in MCM-41 at $T = 0.388$ K. Signal at filling F3 minus that at F2 at the indicated wave vector transfers q are shown. Solid line is a fit of Eq. (1) to the phonon-roton peak.

There is an interesting feature in the scattering intensity shown in Fig. 8 and at lower q values ($q \leqslant 1.65$ Å^{-1}). This is a broad peak in the intensity at $\omega = 0.4 - 0.5$ meV independent of q. This suggests the existence of a dispersionless excitation. Because of uncertainties in background and elastic scattering reaching up to this energy range, it is difficult to quantify the intensity associated with this ''dispersionless mode.'' Further investigation of the low wave vector region is in progress from both an experimental and theoretical point of view.

E. Temperature dependence

In Figs. 10–12, we present results for the temperature dependence of the phonon-roton parameters Z_q, Γ_q, and ω_q for three q values between the maxon and the roton regions. As the temperature increases, the error associated with the parameters generally increases. This is because, as the single excitation peak broadens, it is more difficult to isolate the single excitation component of $S(Q,\omega)$ unambiguously. Also, given our cell design, there is some loss of the liquid ^{4}He from the MCM-41 sample as temperature increases. Some general trends can, however, be identified. The intensity in the single excitation peak (Z_q) clearly decreases with increasing temperature. The half width Γ_q increases with temperature above 1.2 K. Note that the instrument resolution is approximately 0.10 meV so that no change in Γ_q can be observed for $\Gamma_q \leqslant 0.05$ meV. The Γ_q generally decreases with increasing temperature as expected. The temperature change of Γ_q and ω_q at the roton q in the bulk[47] is shown by the dotted line. Essentially, the temperature dependence of Γ_q and ω_q in MCM-41 is the same as in the bulk within the present rather large errors bars.

IV. SUMMARY AND DISCUSSION

The excitations of superfluid ^{4}He confined in several porous media such as aerogel,[15–25] xerogel,[26,27] Vycor,[25,28,29] and 25 Å Geltech silica[30,31] have been observed in the past five years. Our goal in the present measurements is to observe the excitations in a porous media that has regular (cylindrical shaped) pores of small and well determined diameter (32 Å $\pm$ 3 Å). A second goal was to characterize the media and the ^{4}He inside the cylinders as a function of filling more fully than has generally been done in the past. This was done using pressure isotherm measurements, x-ray measurements, and exploratory inelastic neutron scattering measurements. In this way the physical origin of the excitations could be better identified and related to the location and state of the adsorbed ^{4}He.

The first 60% (24 mmol/g) of ^{4}He entering the MCM-41 has very low vapor pressure characteristic of layers very

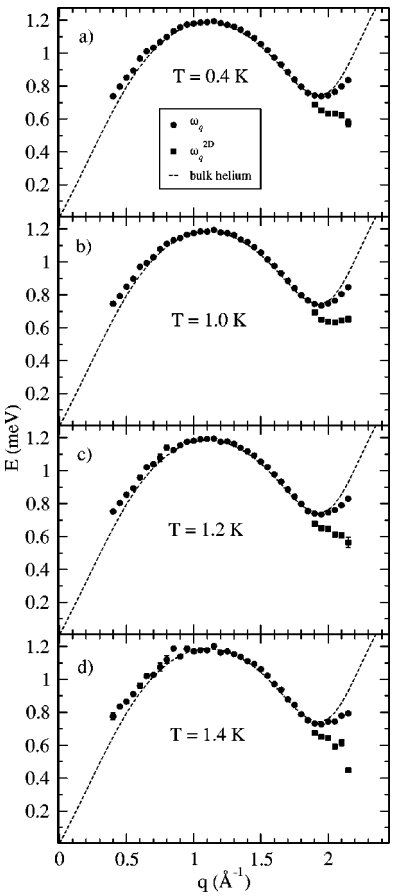

FIG. 9. Results for the fit parameters ω_q and ω_q^{2D} at indicated temperatures.

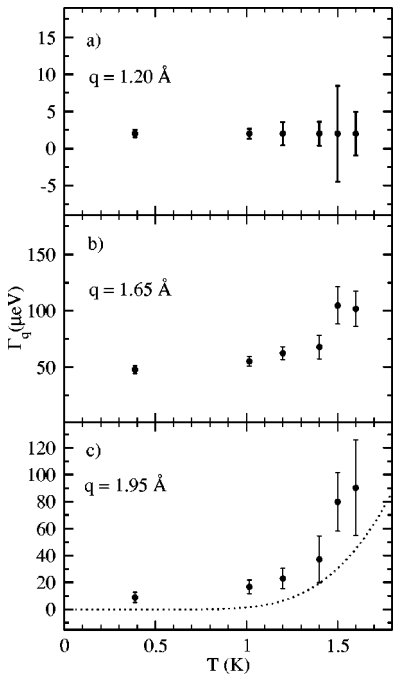

FIG. 11. Results for the fit parameter Γ_q at the indicated q are shown vs temperature. The dotted line in (c) represents results for bulk helium (Ref. 47).

tightly bound to the media walls. This tightly bound ^{4}He does not support any excitations in the energy range investigated here ($0.25\ \text{meV} \leqslant \omega \leqslant 2.0\ \text{meV}$). The subsequent 4 mmol/g of ^{4}He added is still tightly bound but less so and probably forms (or completes) liquid layers. It supports a broad mode peaked at energy $\omega \approx 0.7$ meV. This scattering is

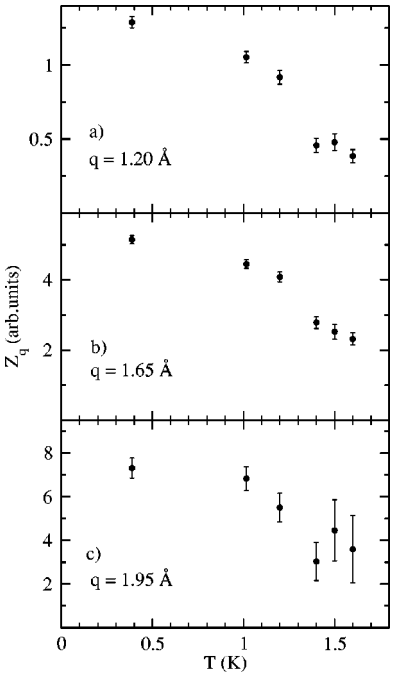

FIG. 10. The intensity in the phonon-roton mode Z_q vs temperature at the q indicated.

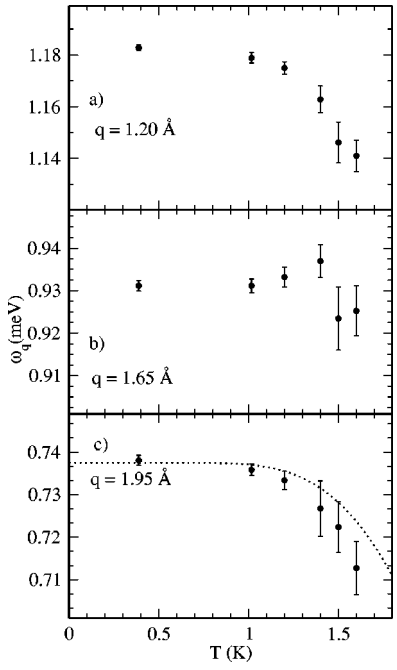

FIG. 12. Results for the fit parameter ω_q at the indicated q are shown vs temperature. Dotted line in (c) represents results for bulk helium (Ref. 47).

consistent with scattering from a ripplon propagating on the free surface of the liquid layer.

Since the MCM-41 is a powder with random orientation of the cylinders, we expect to observe the density of states of the ripplon mode. When the ripplon is observed, the MCM-41 is 70% full (28 mmol/g) and is well described by a simple model consisting of two layers of ^{4}He on the media walls. The ripplon mode disappears after further liquid ^{4}He is added and the free surface is removed. Ripplons have been clearly observed on the free surface of superfluid ^{4}He on graphite.[32,43] However, they have not been observed before on the free surface of superfluid ^{4}He inside a porous medium. Broad scattering intensity was observed at comparable fillings of 25 Å Geltech silica but the intensity was much weaker than observed here and the intensity continued to be observed at higher fillings. Ripplons may be observed in MCM-41 because the surface of the cylinders is smoother (flatter) than in any other porous media investigated to date.

The next approximately 17% of ^{4}He enters MCM-41 as a liquid displaying capillary condensation. In the wave vector range investigated here ($0.4\ \text{Å}^{-1} \leqslant q \leqslant 2.15\ \text{Å}^{-1}$), this liquid ^{4}He (presumably superfluid at low temperatures) supports well defined phonon-roton excitations. The energies and lifetimes of these excitations up to $T=1.6$ K are the same as observed in the bulk within present experimental precision. There is some indication that the phonon energies in MCM-41 at wave vector $q \leqslant 0.5\ \text{Å}^{-1}$ lie above the bulk values increasingly so as q is reduced. This is being investigated further and will be the topic of a separate publication. Accurate measurements of the phonon-roton energies and lifetimes at higher temperatures were not possible because of the small volume of liquid ^{4}He in the present sample. Thus as observed in other porous media, at full or near full filling, the phonon-roton energies and lifetimes of superfluid ^{4}He in MCM-41 are the same as in the bulk within measured precision.

For wave vectors in the roton region ($1.95\ \text{Å}^{-1} \leqslant q \leqslant 2.15\ \text{Å}^{-1}$) we observe additional broad intensity below the $p-r$ peak. This is interpreted as a layer mode propagating in the liquid close to the media walls, as observed in aerogel[24] and other media.[28,31] It is the existence of this mode which distinguishes the response of superfluid ^{4}He in porous media from that in the bulk. Thus the phonon-roton and layer modes observed here in MCM-41 are the same as observed in other porous media except in the phonon region at low wave vector.

It is interesting that we did not observe any identifiable multiple scattering from ^{4}He in MCM-41. Multiple scattering in this context consists of an inelastic scattering from the ^{4}He plus an elastic scattering from the media. Multiple scattering was observed in all other porous media not grown with deuterated materials.[16,17,19,21] While care was taken to clean and evacuate the MCM-41 carefully, the small intensity of multiple scattering is probably because the amount of liquid ^{4}He in the sample was very small. In fact, the amount of capillary condensed liquid ^{4}He is $N_{cc}=7$ mmol g^{-1}. If this has a density $\rho_\lambda = 36.526$ mmol cm^{-3}, it would correspond to a specific liquid helium volume of 0.192 cm^3 g^{-1}. The liquid ^{4}He amount studied in this research would then be 0.36 cm^3.

ACKNOWLEDGMENTS

We thank M. Soulard (Laboratoire de matériaux minéraux, Mulhouse, France) for synthesis and characterization of the MCM-41 sample used in this research. We thank B. Fåk, J. Patarin, N. Dupont-Palovski, and P. Averbuch for advice and scientific discussion. F.A. thanks M.-C. Bellissent-Funel for full scientific support. We wish to gratefully aknowledge X. Agostini, D. Louçano, A. Gabriel, P. Boutrouille, A. Buteau, M. De Palma, F. Thomas, S. Jenkins, S. Pujol, P. Pari, and P. Bourget for inestimable technical support. This work was supported by the European Community through the TMR Grant No. ERB4001GT973305 and partially by National Science Foundation Grant No. DMR-0115663.

*Electronic address: albergam@ill.fr
†Electronic address: bossy@grenoble.cnrs.fr
‡Electronic address: glyde@udel.edu
§Electronic address: dianoux@ill.fr

[1] J. D. Reppy, J. Low Temp. Phys. **87**, 205 (1992).
[2] M. P. A. Fisher, P. B. Weichman, G. Grinstein, and D. S. Fisher, Phys. Rev. B **40**, 546 (1989).
[3] G. E. Astrakharchik, J. Boronat, J. Casulleras, and S. Giorgini, Phys. Rev. A **66**, 023603 (2002).
[4] G. Blatter, M. V. Feigel'man, V. B. Geshkenbein, A. I. Larkin, and V. M. Vinokur, Rev. Mod. Phys. **66**, 1125 (1994).
[5] U. C. Tauber and D. R. Nelson, Phys. Rep. **289**, 157 (1997).
[6] N. Trivedi, A. Ghosal, and M. Randeria, Int. J. Mod. Phys. B **15**, 1347 (2001).
[7] N. Markovíc, C. Christiansen, A. M. Mack, W. H. Huber, and A. M. Goldman, Phys. Rev. B **60**, 4320 (1999).
[8] A. P. Y. Wong and M. H. W. Chan, Phys. Rev. Lett. **65**, 2567 (1990).
[9] N. Mulders, R. Mehrotra, L. S. Goldner, and G. Ahlers, Phys. Rev. Lett. **67**, 695 (1991).
[10] M. Larson, N. Mulders, and G. Ahlers, Phys. Rev. Lett. **68**, 3896 (1992).
[11] M. Larson, N. Mulders, R. Mehrotra, L. S. Goldner, and G. Ahlers, J. Low Temp. Phys. **89**, 79 (1992).
[12] G. K. S. Wong, P. A. Crowell, H. A. Cho, and J. D. Reppy, Phys. Rev. B **48**, 3858 (1993).
[13] R. Maynard and G. Deutscher, Europhys. Lett. **10**, 257 (1989).
[14] J. D. Reppy, B. C. Crooker, B. Hebral, A. D. Corwin, J. He, and G. M. Zassenhaus, Phys. Rev. Lett. **84**, 2060 (2000).
[15] J. D. Kinder, G. Coddens, and R. Millet, Z. Phys. B: Condens. Matter **95**, 511 (1994).
[16] G. Coddens, J. D. Kinder, and R. Millet, J. Non-Cryst. Solids **188**, 41 (1995).
[17] M. R. Gibbs, P. E. Sokol, R. T. Azuah, W. G. Stirling, and M. A. Adams, Physica B **213-214**, 462 (1995).
[18] P. E. Sokol, M. R. Gibbs, W. G. Stirling, R. T. Azuah, and M. A. Adams, Nature (London) **379**, 616 (1996).
[19] M. R. Gibbs, P. E. Sokol, W. G. Stirling, R. T. Azuah, and M. A.

Adams, J. Low Temp. Phys. **107**, 33 (1997).
[20] R. M. Dimeo, P. E. Sokol, D. W. Brown, C. R. Anderson, W. G. Stirling, M. A. Adams, S. H. Lee, C. Rutiser, and S. Komarneni, Phys. Rev. Lett. **79**, 5274 (1997).
[21] O. Plantevin, B. Fåk, H. R. Glyde, J. Bossy, and J. R. Beamish, Phys. Rev. B **57**, 10 775 (1998).
[22] R. T. Azuah, H. R. Glyde, J. R. Beamish, and M. A. Adams, J. Low Temp. Phys. **117**, 113 (1999).
[23] C. R. Anderson, K. H. Andersen, J. Bossy, W. G. Stirling, R. M. Dimeo, P. E. Sokol, J. C. Cook, and D. W. Brown, Phys. Rev. B **59**, 13 588 (1999).
[24] B. Fåk, O. Plantevin, H. R. Glyde, and N. Mulders, Phys. Rev. Lett. **85**, 3886 (2000).
[25] O. Plantevin, B. Fåk, H. R. Glyde, N. Mulders, J. Bossy, G. Coddens, and H. Schober, Phys. Rev. B **63**, 2245081 (2001).
[26] C. R. Anderson, W. G. Stirling, K. H. Andersen, P. E. Sokol, and R. M. Dimeo, Physica B **276-278**, 820 (2000).
[27] C. R. Anderson, K. H. Andersen, W. G. Stirling, P. E. Sokol, and R. M. Dimeo, Phys. Rev. B **65**, 174509 (2002).
[28] R. M. Dimeo, P. E. Sokol, C. R. Anderson, W. G. Stirling, K. H. Andersen, and M. A. Adams, Phys. Rev. Lett. **81**, 5860 (1998).
[29] H. R. Glyde, O. Plantevin, B. Fåk, G. Coddens, P. S. Danielson, and H. Schober, Phys. Rev. Lett. **84**, 2646 (2000).
[30] O. Plantevin, B. Fåk, and H. R. Glyde, J. Phys. IV **10**, 177 (2000).
[31] O. Plantevin, H. R. Glyde, B. Fåk, J. Bossy, F. Albergamo, N. Mulders, and H. Schober, Phys. Rev. B **65**, 224505/1 (2002).
[32] H. J. Lauter, H. Godfrin, and P. Leiderer, J. Low Temp. Phys. **87**, 425 (1992).
[33] H. R. Glyde, B. Fåk, N. H. van Dijk, H. Godfrin, K. Guckelsberger, and R. Scherm, Phys. Rev. B **61**, 1421 (2000).
[34] R. T. Azuah, H. R. Glyde, R. Scherm, N. Mulders, and B. Fåk, J. Low Temp. Phys. (to be published).
[35] A. Corma, Q. Kan, M. T. Navarro, J. Pérez-Pariente, and F. Rey, Chem. Mater. **9**, 2123 (1997).
[36] E. P. Barrett, L. G. Joyner, and P. P. Halenda, J. Am. Chem. Soc. **73**, 373 (1951).
[37] S. Brunauer, P. H. Emmet, and E. Teller, J. Am. Chem. Soc. **60**, 309 (1938).
[38] K. Carneiro, W. D. Ellenson, L. Passell, J. P. McTague, and H. Taub, Phys. Rev. Lett. **37**, 1695 (1976).
[39] W. Thomlinson, J. A. Tarvin, and L. Passell, Phys. Rev. Lett. **44**, 266 (1980).
[40] H. J. Lauter, H. P. Schildberg, H. Godfrin, H. Wiechert, and R. Haensel, Can. J. Phys. **65**, 1435 (1987).
[41] R. D. McCarthy (unpublished).
[42] R. A. Watkins, W. L. Taylor, and W. J. Haubach, J. Chem. Phys. **46**, 1007 (1967).
[43] H. J. Lauter, H. Godfrin, V. L. P. Frank, and P. Leiderer, Phys. Rev. Lett. **68**, 2484 (1992).
[44] D. O. Edwards, J. R. Eckardt, and F. M. Gasparini, Phys. Rev. A **9**, 2070 (1974).
[45] D. O. Edwards and W. F. Saam, in *Progress in Low Temperature Physics*, edited by D. Brewer (North Holland, Amsterdam, 1978). Vol. VII A, Chap. 4, pp. 283–369.
[46] A. Lastri, F. Dalfovo, L. Pitaevskii, and S. Stringari, J. Low Temp. Phys. **98**, 227 (1995).
[47] K. H. Andersen, W. G. Stirling, R. Scherm, A. Stunault, B. Fåk, H. Godfrin, and A. J. Dianoux, J. Phys.: Condens. Matter **6**, 821 (1994).
[48] See, for instance, http://www.ill.fr/tas/practical/orange_man.htm